

# Hierarchical semantic composition of biosimulation models using bond graphs

Nilofar Shahidi<sup>1\*</sup>, Michael Pan<sup>2,3</sup>, Soroush Safaei<sup>1</sup>, Kenneth Tran<sup>1</sup>, Edmund J. Crampin<sup>2,3</sup>, David P. Nickerson<sup>1</sup>

**1** Auckland Bioengineering Institute, The University of Auckland, Auckland, New Zealand

**2** Systems Biology Laboratory, School of Mathematics and Statistics, and Department of Biomedical Engineering, University of Melbourne, Melbourne, Victoria, Australia

**3** ARC Centre of Excellence in Convergent Bio-Nano Science and Technology, Faculty of Engineering and Information Technology, University of Melbourne, Melbourne, Victoria, Australia

\* E-mail: [nsha457@aucklanduni.ac.nz](mailto:nsha457@aucklanduni.ac.nz) (NS)

## Abstract

Simulating complex biological and physiological systems and predicting their behaviours under different conditions remains challenging. Breaking systems into smaller and more manageable modules can address this challenge, assisting both model development and simulation. Nevertheless, existing computational models in biology and physiology are often not modular and therefore difficult to assemble into larger models. Even when this is possible, the resulting model may not be useful due to inconsistencies either with the laws of physics or the physiological behaviour of the system. Here, we propose a general methodology for composing models, combining the energy-based bond graph approach with semantics-based annotations. This approach improves model composition and ensures that a composite model is physically plausible. As an example, we demonstrate this approach to automated model composition using a model of human arterial circulation. The major benefit is that modellers can spend more time on

understanding the behaviour of complex biological and physiological systems and less time wrangling with model composition.

## Author summary

Biological and physiological systems usually involve multiple underlying processes, mechanisms, structures, and phenomena, referred to here as sub-systems. Modelling the whole system every time from scratch requires a huge amount of effort. An alternative is to model each sub-system in a modular fashion, *i.e.*, containing meaningful interfaces for connecting to other modules. Such modules are readily combined to produce a whole-system model. For the combined model to be consistent, modules must be described using the same modelling scheme. One way to achieve this is to use energy-based models that are consistent with the conservation laws of physics. Here, we present an approach that achieves this using bond graphs, which allows modules to be combined faster and more efficiently. First, physically plausible modules are generated using a small number of template modules. Then a meaningful interface is added to each module to automate connection. This approach is illustrated by applying this method to an existing model of the circulatory system and verifying the results against the reference model.

## Introduction

Mathematical models have long been used to study biological systems and predict their behaviours [1,2]. However, the expansion of biological models to bridge between cells and organs demands reusable and comprehensible existing models to avoid the repetitive work of recreating them [3,4]. Constructing a complex model by composing various well-defined sub-models (modularisation) helps researchers handle this complexity [5], facilitates model composition and promotes model sharing [6–8].

Mathematical modelling in the context of biology was first intended to simplify the analysis of biological and physiological processes and systems. Such models are generally applicable in the context in which they were developed, which determines how complicated a model should be [9,10]. While such single-purpose models are often

computationally efficient, they cannot be utilised to simulate different biological conditions [10]. This occurs because single-purpose models only give the investigator an insight into the specific data from which they were derived, and are unable to predict beyond that given knowledge [11, 12]. Complex, fully detailed models may be valid under more physiological conditions, but are often challenging to comprehend and simulate [4]. In the end, we need a compromise between complexity and simplicity while capturing the main physical features of a system.

In recent years, as the Physiome ([www.physiomeproject.org](http://www.physiomeproject.org)) and Virtual Physiological Human (VPH) ([www.vph-institute.org](http://www.vph-institute.org)) projects have demonstrated, initial steps have been taken to construct more realistic models able to describe almost every system in the body (from cell to organs) [13, 14]. By assembling these models (model composition), one can construct a model of the whole or part of the human body. However, many computational models are not expressed in a uniform format, making it difficult - if not impossible - to assemble them [15]. Most existing mathematical modelling methods are not flexible enough for modularisation and require significant editing of the equations and code after recombination the modules [16]. Establishing a link between the physiological processes and biological systems at any level of operation in the body requires multiscale modelling [17, 18]. This calls for a standardised and general-purpose platform, which once implemented, can help scientists conduct *in silico* experiments and examine hypotheses on a virtual body model [19].

Throughout the natural world, *energy* is always conserved [20]. Therefore, if energy is selected as the exchange variable in the models, especially in composing multiple models across different domains of physics, it ensures that all the individual models are thermodynamically and physically consistent [21, 22]. Bond graphs provide an energy-based and general-purpose modelling framework that ensures models obey thermodynamic and physical principles [22, 23]. Bond graphs were invented by Henry Paynter and were initially meant to be used in mechanical systems [24]. In bond graphs, all systems are reduced to a graphical representation in which physical components are connected by a network of bonds (graphically represented as half-arrows) and junctions. Bonds carry two physical co-variables: potential (in Joule per quantity) and flow (in quantity per second). Noting that the product of potential and flow is power (in Joules per second), bonds are energy-conserving. Junctions either share a common potential

(shown by ‘0’) or share a common flow (shown by ‘1’). These notations are analogous to the Kirchhoff’s laws in electrical circuits, equilibrium of forces in mechanical systems, and stoichiometry balance in chemical reactions [25]. Since these conservation laws in different domains follow the same mathematical principles, they can be represented by generalised equations using bond graphs.

The application of bond graphs to biochemical processes was proposed by Oster et al. [26] and has recently been advanced by Gawthrop and Crampin [4, 22]. The bond graph description of a biophysical model produces components that have physical and biophysical interpretations, assisting a better understanding of the system. Once each module is represented in bond graph form, correct coupling between modules is straightforward, and the resultant model is itself a bond graph and hence physically consistent [6].

Endeavours to automate model composition have led to a number of proposed composition platforms, standards, and outlines [15, 27–30], each suitable for a specific set of modelling tasks. Automating this procedure aids the investigators with faster and more reliable model composition in which the linking points between the modules can be automatically detected. However, at present, many biological models do not consider fundamental physical and thermodynamic principles [23], often violating conservation of mass and energy in the underlying equations [31]. Together these produce inconsistencies when models are composed [19]. Semantically enriched bond graph modules would enable the automation of model composition, as each module can be confidently linked to others via common annotated components [30]. There has been a consensus among the Physiome Project and the VPH to label the mathematical contents of the computational models with meaningful semantics, known as annotations [32]. In this way, not only do models contain biological knowledge that is readily interpretable by everyone, but also they become accessible and reusable [14, 32].

Representing the modules in the Cellular modelling Markup Language (CellML) format, meets these standards [5]. CellML is a machine-readable XML-based language which relies on modular modelling and allows reusing components from other models which facilitates model construction. It also reads and runs the simulation for the models containing annotations.

CellML models can be merged using SemGen (available from:

<https://github.com/SemBioProcess/SemGen/releases>). SemGen is a free  
Java-based application designed for annotating, merging, and extracting biosimulation  
models encoded in CellML [33], Systems Biology Markup Language (SBML) [34] and  
JSim's Mathematical Modelling Language (MML) [35,36]. It generates the semantic  
annotations as Resource Description Framework (RDF) triples  
(<https://www.w3.org/RDF>) and adds them to the model code. Unlike other  
composition approaches that rely on pre-defined module interfaces for coupling,  
SemGen uses a 'white box' approach in which any element of the modules can be  
selected as joint components by constructing required mappings between the module  
elements [37]. In contrast, for example, in 'black box' compositions, the internal  
components of the blocks are hidden. Only the input/output variables are available for  
the user for coupling the modules [3]. One of the disadvantages of this approach in the  
biological context is that usually the majority of the entities in a model are potentially  
capable of being considered as coupling ports. Therefore, using the 'black box'  
configuration is not compatible with our modelling purposes.

Here, we demonstrate a general method for semantics-based automated model  
composition using bond graphs, which enables rapid construction of whole body  
multiscale models. To demonstrate this, we construct and combine simplified, reusable  
bond graph modules for the Anatomically Detailed Arterial Network (ADAN) open-loop  
circulatory model based on existing work by Safaei et al. [25,38]. The ADAN model,  
first mathematically developed as a partial differential equation (PDE) model by  
Watanabe et al. [39], anatomically and physiologically describes the arterial network in  
terms of segments and branches in which blood flow is simulated. Safaei et al. have  
since developed physically-plausible lumped parameter models based on this work. The  
ADAN model for the arterial network for the entire body is called ADAN closed-loop  
whereas the reduced version of this model is called ADAN open-loop model, which  
represents the arterial network of the body except for the cerebral system. To generate  
the ADAN open-loop model, we employ SemGen's semantics-based merging tool to  
capture the common entities across the modules and provide a list of likely variables for  
composition. Simulation results produced by the assembled model and comparisons to  
the ADAN open-loop bond graph model are presented and discussed, along with  
possible improvements to the semantics-based model composition approach.

## Materials and methods

108

This section discusses the composition of CellML models using SemGen's merging tool  
to reconstruct the ADAN open-loop model of the arterial system. Particularly, we will  
show that we only need three templates to generate the 86 vessel segments of the  
ADAN open-loop model. Later, we will demonstrate the potential for reuse in the case  
of having similar sections in a system (as in the right and left limbs). Ultimately, the  
quantities for all the biological entities can also be mapped to the model variables using  
the SemGen merger tool. Our approach is summarised in Fig 1, illustrating the  
flowchart of the modelling procedure. SemGen annotator and merger tools are discussed  
further in [37].

109

110

111

112

113

114

115

116

117

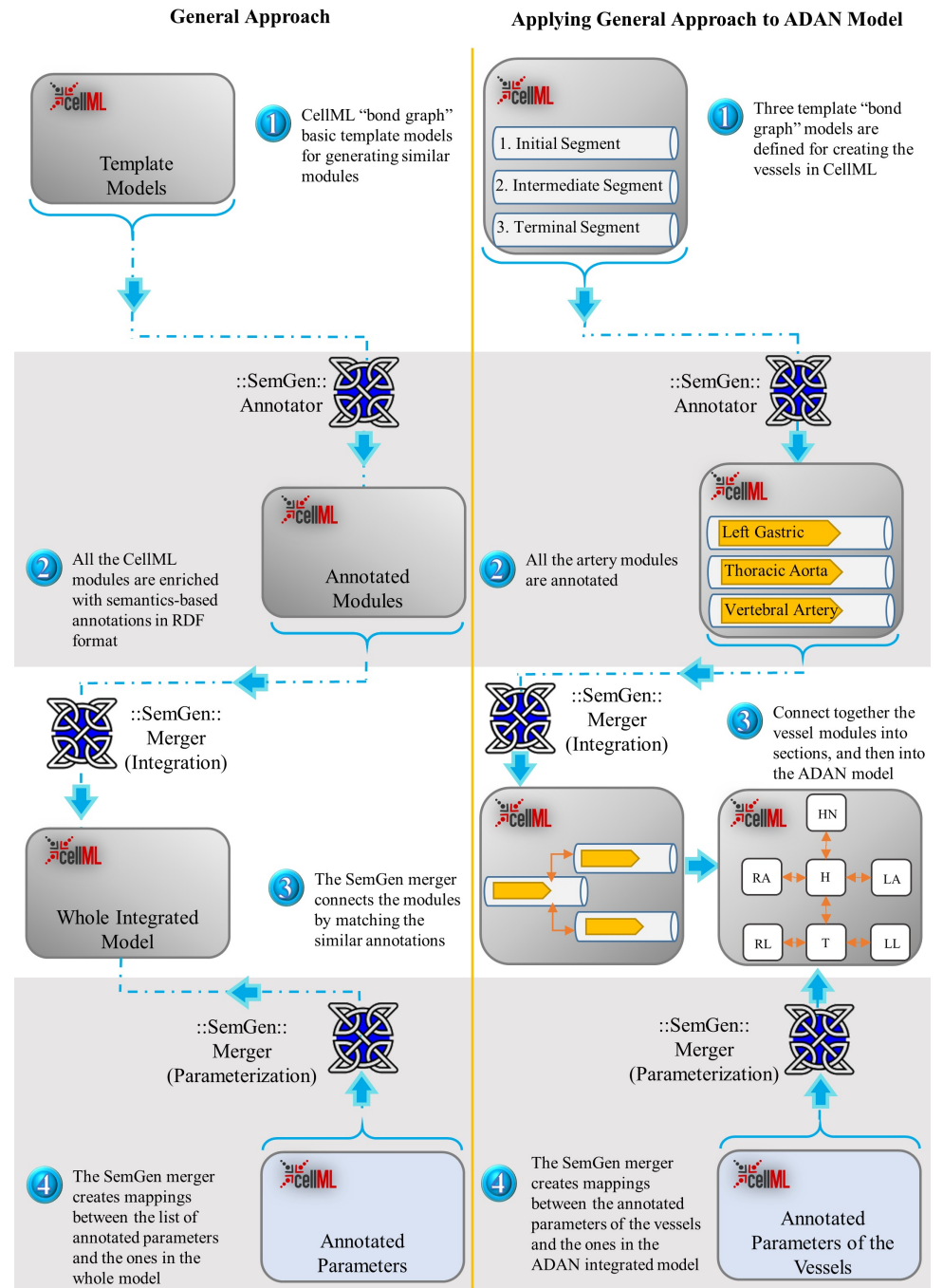


**Fig 1. Flowchart of the semantics-based automated model composition method.** The left column illustrates the general approach in the integration of bond graph models in CellML using SemGen, and the right column shows the same procedure specific to the ADAN circulation model. In both approaches, the bond graph models are created based on template models (1), and annotated using the SemGen Annotator (2). Later, depending on whether the system has similar larger compartments or any symmetry, the SemGen merger tool joins the modules in a number of steps (3). The amounts for the symbolic model parameters are allocated from a CellML file containing the annotated parameters and their values (4). In stage (3): HN: Head and Neck, H: Heart, RA: Right Arm, LA: Left Arm, T: Trunk, RL: Right Leg, LL: Left Leg.

## Semantic model composition using SemGen

SemGen has been used to integrate several mathematical models by treating them as modules [35,40]. However, SemGen does not currently have the capability to edit the equations in the models being merged [41]. Thus, conflicts may arise while coupling the mathematical models, requiring post-merging adjustments in equations. Often, these post-merging modifications are error-prone, prolonged [40,42] and require a context-specific knowledge of the underlying equations. Thus, although SemGen has facilitated mathematical model composition, it is still reliant on the modeller's decisions to produce an integrated biological model which produces feasible results [35,40,42,43].

To avoid this, we propose using the bond graph approach for creating the modules. Describing biological and physiological systems in terms of bond graphs in CellML allows us to take the advantage of both the energy-based and hierarchical nature of the bond graph approach and the convenient semi-automated merging tool of SemGen. Existing merging tools like SemGen do not consider physical constraints, while the bond graph framework imposes these constraints to the system. Consequently, by defining the CellML modules using bond graphs, the network structure allows conservation equations to be systematically updated when merging models. This allows us to avoid manually mapping the relationships between the sub-models in CellML. Furthermore, representing the bond graph models in CellML also lets us create mappings via SemGen between different variables and parameters, thus avoiding multiple definitions of the same physiological parameter or variable.

### Human arterial network model

Safaei et al. [25] developed a detailed CellML model of the human arterial network using bond graphs, based on the ADAN model. The model was created by defining manual mappings between different types of bond graph vessel models. For a large model, these manual mappings are time-consuming and require a significant amount of work. Here, we demonstrate that the same can be achieved in an automated manner using the SemGen merger tool and intrinsic hierarchical properties of bond graphs. We also demonstrate that adding an auxiliary variable to each bond graph module in CellML enables coupling of modules via SemGen. Thereby, the creation of complex



models becomes simpler, systematic, hence time-efficient, and less error-prone. 148

Each vessel segment can be modelled in bond graphs using  $R$ ,  $C$ , and  $I$  components, 149  
representing the viscous resistance, vessel wall compliance, and mass inertial effect in 150  
fluid mechanics, respectively [25]. Here, 151

- The potential variable is  $u$ , the energy density or pressure ( $\text{J}/\text{m}^3$ ). The flow 152  
variable is  $v$ , the fluid volumetric flow ( $\text{m}^3/\text{s}$ ); 153
- Segment compliances are defined using  $C$  components, given by the constitutive 154  
relation  $u = q/C$ , where  $q$  ( $\text{m}^3$ ) is the excess volume caused by dilation of the 155  
segment and  $C$  is the vessel wall compliance; 156
- Inertial storage is defined using an  $I$  component with a constitutive relation 157  
 $u = Ia$ , where  $a = \frac{dv}{dt}$  is the flow rate and  $I$  is the mass inertial effect; 158
- $R$  represents the viscous resistance with a constitutive relation  $u = Rv$ . 159

The relationships between the bond graph elements are determined by the energy 160  
conservation laws in the network structure and the constitutive relations within 161  
components, which make bond graph models physically coherent. The two conjugate 162  
variables indicate the flow of energy between the bond graph elements; ‘potential’ and 163  
‘flow’ which enable the bidirectional flow of information [44,45]. A more extensive 164  
presentation of bond graph theory, and several examples can also be found in [46,47]. 165

The parameters of each segment were calculated in terms of vessel properties using 166  
the equations: 167

$$R = \frac{8\nu l}{\pi r^4} \quad (1)$$

$$I = \frac{\rho l}{\pi r^2} \quad (2)$$

$$C = \frac{2\pi r^3 l}{Eh}. \quad (3)$$

The biological and geometric interpretations of the arterial parameters used in Eqs 168  
(1), (2) and (3) are given in Table 1. 169

**Table 1. Vessel properties description.**

Vascular Properties			
Parameter	Definition	Value	Unit
$\nu$	Blood viscosity	0.004	$\text{J.s.m}^{-3}$
$\rho$	Blood density	1050	$\text{J.s}^2.\text{m}^{-5}$
$E$	Young's modulus	$0.4 \times 10^6$	$\text{J.m}^{-3}$
$l$	Length	(Segment specific)	m
$r$	Radius		m
$h$	Wall thickness	$r(ae^{br} + ce^{dr})$	m
$a$	Fitting coefficient	0.2802	–
$b$	Fitting coefficient	–505.3	$\text{m}^{-1}$
$c$	Fitting coefficient	0.1324	–
$d$	Fitting coefficient	–11.14	$\text{m}^{-1}$

The wall thickness constants ( $a, b, c, d$ ) are mathematical fitting parameters and are considered to be the same for all the vessels.

The dependency of the vessel wall thickness and its radius is logarithmic, as discussed in [48] and later in [49] and [25].

## Template modules

Vessels are represented by generic template bond graph modules based on their mechanical properties. Each non-branching vessel segment is composed of a parallel  $C$ , an  $R$  and  $I$  in series, connected by bonds (Fig 2). To emphasise the concept of sharing common potential and common flow in ‘0’ and ‘1’ junctions, we denote them as ‘0 :  $u$ ’ and ‘1 :  $v$ ’, respectively, in which  $u$  stands for potential and  $v$  stands for flow.

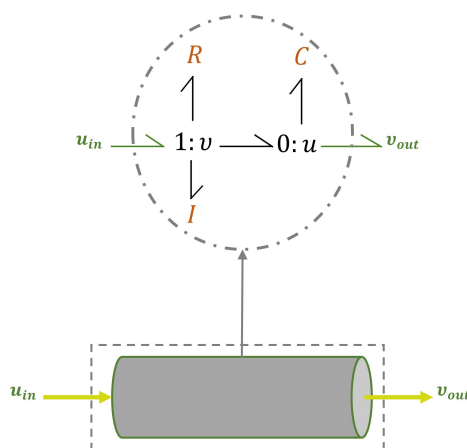


**Fig 2. Bond graph representation of a non-branching vessel.**  $C$ ,  $R$  and  $I$  components show the mechanical properties of a vessel segment.

Depending on whether a vessel is located adjacent to the source of flow ( $S_f$ ), at a terminal point, or in the middle of the vessels network (bifurcating or not), we modify the original configuration of Fig 2 and define three types of modules: initial, intermediate, and terminal. These three types of bond graph modules are described in Fig 3.  $R_A$  and  $R_B$  in Fig 3A and Fig 3B account for the viscoelastic effect of the vessel wall.

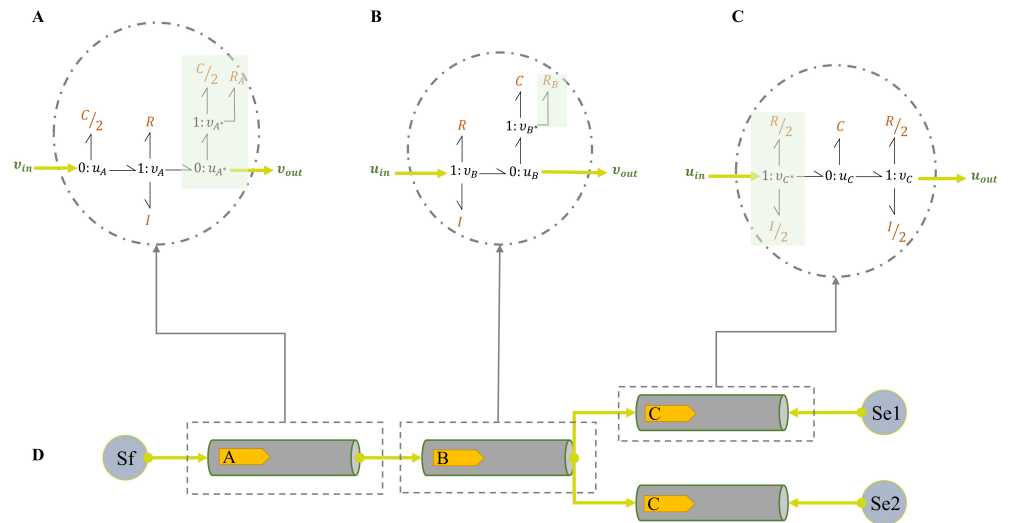


**Fig 3. Required bond graph template modules for the vessels in the ADAN open-loop model.** Depending on the type and location of a vessel, three template modules can be proposed: (A) initial segment; (B) intermediate segment; (C) terminal segment; (D) the schematic of the segments connections.  $S_f$  and  $\{Se_1, Se_2\}$  are sources of flow and pressure in bond graphs which are *cardiac output* and *venous pressure* in the ADAN open-loop model [25]. The components in green boxes are the added sections to the original bond graph configuration of Fig 2.

To ensure the conservation of mass and energy, potential and flow must obey conservation laws, *i.e.*, the sum of all the energy flows at each junction is zero [47] (*i.e.*, energy is neither created nor destroyed at a junction):

$$\sum_{i=1}^n u_i \cdot v_i = 0 \quad (4)$$

where  $i$  indicates the number of bonds impinging on a junction. Depending on the type of junction, one co-variable is considered fixed in the conservation equations. In a ‘0 :  $u$ ’ junction the potential is fixed; and in a ‘1 :  $v$ ’ junction the flow is fixed. Eqs (5) and (6) are the conservation relations for ‘0 :  $u$ ’ and ‘1 :  $v$ ’ junctions, respectively.

$$\begin{cases} u_1 = u_2 = \dots = u_n, \\ \sum_{i=1}^n v_i = 0 \end{cases} \quad (5)$$

$$\begin{cases} v_1 = v_2 = \dots = v_n, \\ \sum_{i=1}^n u_i = 0 \end{cases} \quad (6)$$

The terminal junctions in each module are selected for coupling with other modules. 191  
 When two modules are coupled, and a bond is added to a junction, there is 192  
 consequently a change in the conservation equations of that junction. For instance, 193  
 consider the modules in Fig 3A and Fig 3B. The conservation equations at their 194  
 terminal junctions would be as in Fig 4. 195

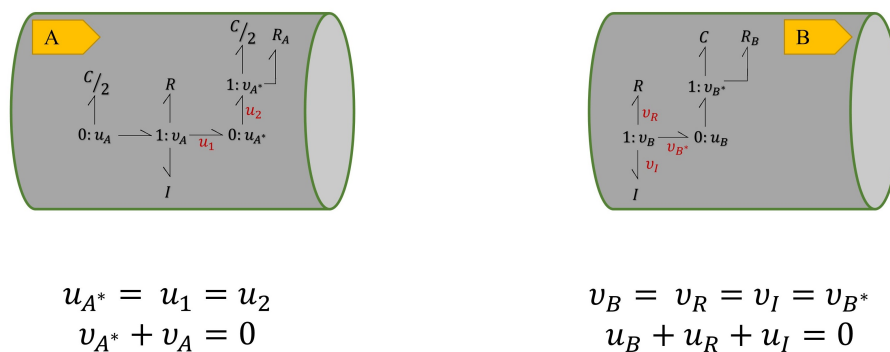


**Fig 4. Conservation equations at the terminal junctions in two bond graph modules.** Equal flows at  $1 : v$  junction and equal potentials at  $0 : u$  junction. The sum of potentials equals to the inward potential in the  $1 : v$  junctions and the sum of flows equals to the outward flow in the  $0 : u$  junctions.

To track the changes to the constitutive equations, we have selected the  $C/2$  and  $R_A$  196  
 components at  $1 : v_{A^*}$  junction in **A**. The constitutive equations in the case of Fig 4 197  
 would be: 198

$$\begin{cases} u_{R_A} = R_A v_{A^*}, \\ u_{C/2} = \frac{2}{C} \frac{dv_{A^*}}{dt}. \end{cases} \quad (7)$$

where based on the conservation laws,  $v_{A^*} = -v_A$ .

By creating an additional bond between the  $0 : u$  junction in **A** and the  $1 : v$  junction in **B**, these two segments can be coupled together. As potential is fixed in a  $0 : u$  junction, an additional bond to the junction means the addition of one flow term in Eq (5). In the same manner adding a bond to a  $1 : v$  junction means an extra potential term in Eq (6). This is illustrated in Fig 5 where the amount of  $v_B$  in **B** is added to the conservation equation at  $0 : u_{A^*}$  junction in **A** and also the amount of  $u_{A^*}$  in **A** is added to the conservation equation at  $1 : v_B$  junction in **B**.

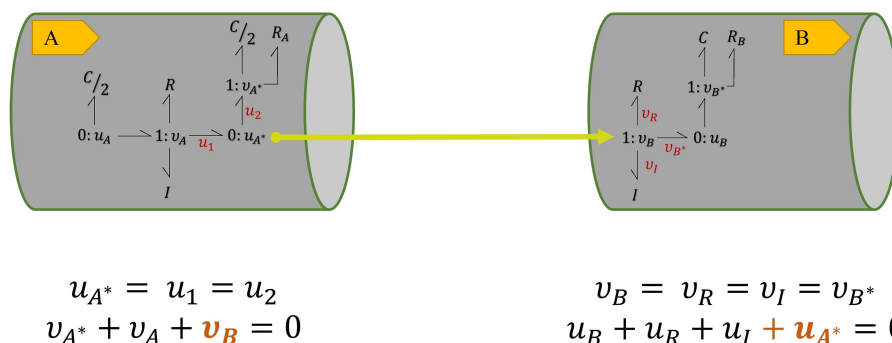


**Fig 5. Conservation equations at the terminal junctions in two coupled bond graph modules.**  $v_B$  in **B** is added to the conservation equation at  $0 : u_{A^*}$  junction in **A** and  $u_{A^*}$  in **A** is added to the conservation equation at  $1 : v_B$  junction in **B**. Each terminal junction's  $v$  or  $u$  in each module is added to the other module's conservation equation, representing the addition of a bond.

By adding a bond between the junctions, the constitutive equations of the components at  $1 : v_{A^*}$  junction in **A** remain as in Eq (7). However, based on the conservation laws in Fig 5,  $v_{A^*}$  would be calculated as  $v_{A^*} = -v_A - v_B$ .

In order to compose models from these modules, we need to impose these changes into the CellML models. To do this, we propose adding auxiliary variables ( $v_x$  or  $u_x$ , depending on the type of the junction) to each module. These auxiliary variables are set to zero by default, so they do not have any impact while the model is running separately. However, when the modules are integrated, we can readily create a mapping between the terminal junctions' known variables ( $v$  or  $u$ , depending on the type of the junction). This is demonstrated in Fig 6.

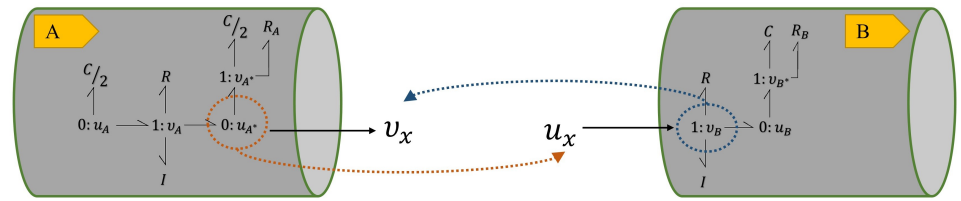


**Fig 6. Bond graph modular connection of the vessel models.**  $v$  in the initial junction of the following module will be mapped to  $v_x$  at the terminal junction of its preceding module. In the same way,  $u$  at the terminal junction of each module will be mapped to  $u_x$  at the initial junction of its following module.  $v_x$  and  $u_x$  are auxiliary variables.

We also need to deal with the case when a vessel is split into two or more branches. We have already stated that for any number of branching or even non-branching vessels, we use a common type of bond graph configuration. In this case, the idea is to impose *a priori* a maximum number of branching occurring in a vessel of the network. Then we create our template module having four  $v_x$  variables (see Fig 7). This creates the generic modules we require for composing the full circulation model.



**Fig 7. The template bond graph module for intermediate vessels in our version of the ADAN open-loop model.** The number of  $v_x$  variables depends on the maximum number of branches occurring in any segment. Here, four auxiliary variables corresponding to four branches are demonstrated.

## The SemGen merger tool

SemGen allows models encoded in CellML and SBML to be composed and is a powerful tool for semantics-based annotations, which enriches the models with the physiological and biological information about the entities and processes. Once modules are annotated, merging becomes easier as SemGen automatically detects the semantic overlaps and suggests to the user a list of identical or similar annotations in both

modules. SemGen can merge only two models at one time. So, for the composition of  $n$  229  
models,  $(n-1)$  merging steps are required. In this paper, we propose a hierarchical 230  
approach for module composition in fractal and repetitive segments in large systems, 231  
which reduces the number of merging tasks significantly. In the ADAN open-loop 232  
vascular model, the vessels can be grouped in seven subdivisions; HEAD AND NECK, 233  
HEART (cardiac output), TRUNK, LEFT ARM, RIGHT ARM, LEFT LEG and RIGHT LEG. 234  
Each subdivision can be created separately by merging the required vessel segments, 235  
and then be put together with other vascular sections. As the vascular segments for the 236  
limbs can be assumed identical, we can wrap the vascular model of a limb as a lumped 237  
module and then reuse it. The schematic of the created lumped modules of the ADAN 238  
open-loop model is illustrated in Fig 8. This lumping method can be generalised and 239  
applied to all types of systems that have similar sections. 240

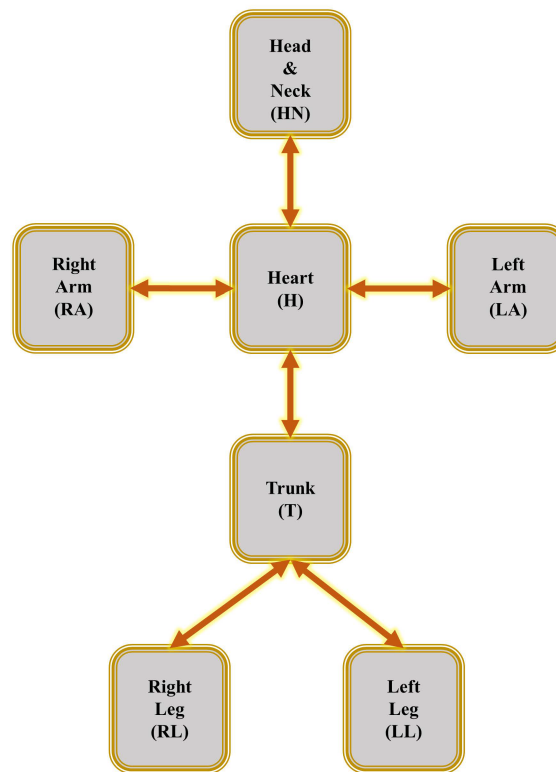


**Fig 8. Lumped modules in the ADAN open-loop model.** These lumped modules will be connected in the final step using the SemGen merger tool to produce the whole ADAN open-loop model.

The series of vessel segments in each lumped module is shown in Figure 9.

241

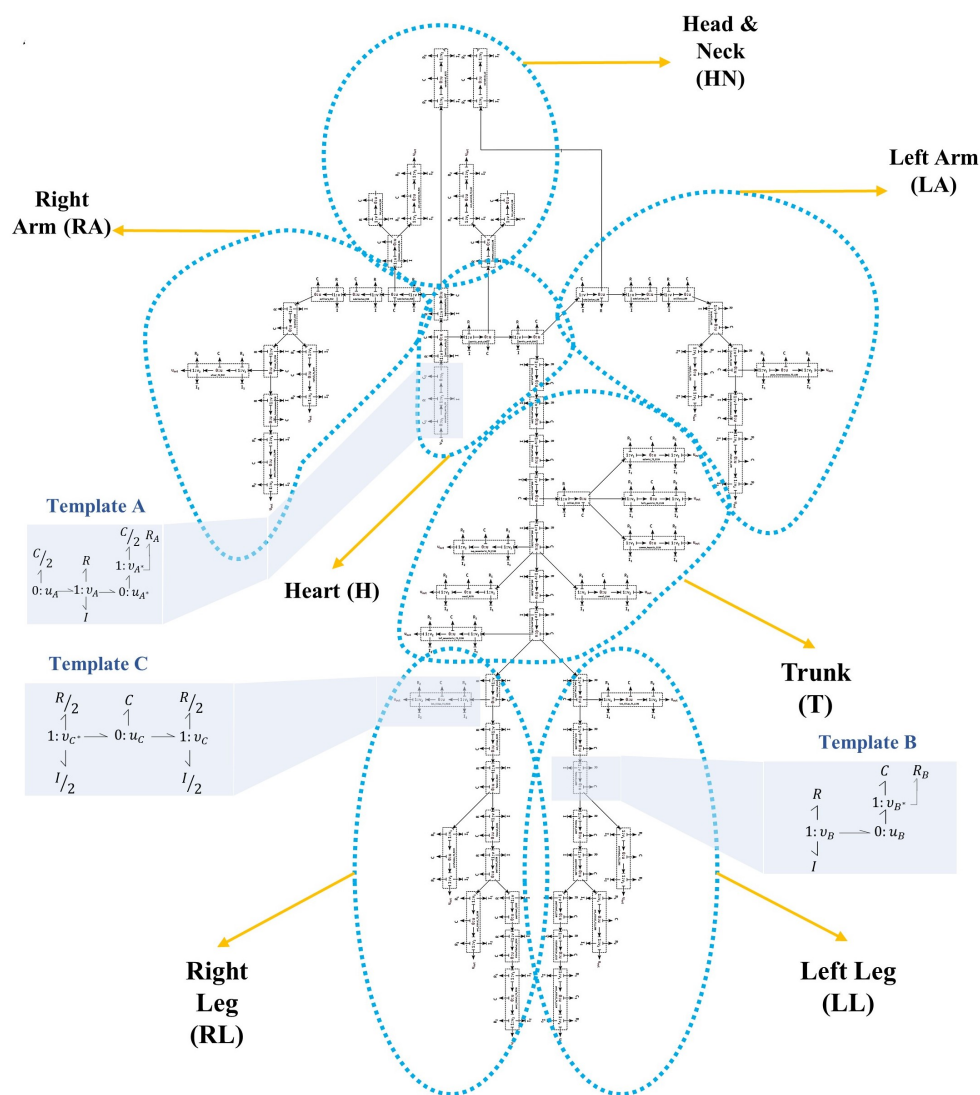


**Fig 9. Vessels network in the ADAN open-loop model.** The blue dashed shapes delineate the segments in each lumped module. The three bond graph templates of Fig 3 are shown in blue boxes for three exemplar segments. The segments network is adopted from [25].

To visualise how the SemGen merger tool is utilised, the merging of two modules is depicted in Fig 10.

242

243



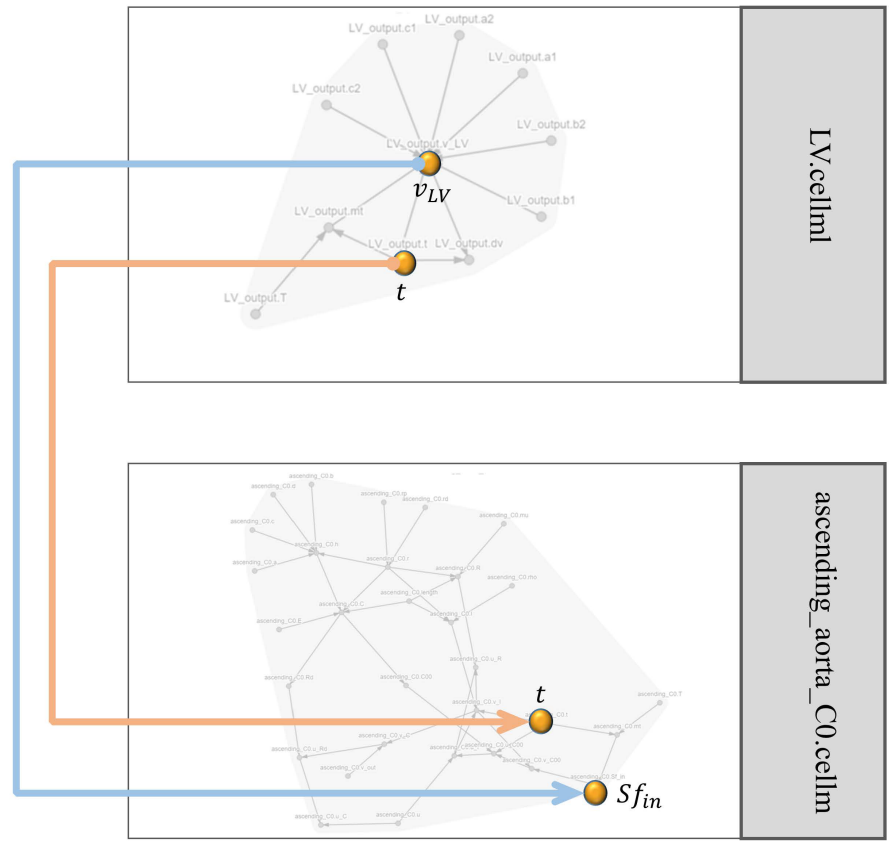


**Fig 10. The SemGen merger tool visualisation for two modules.** The model of left ventricle output flow (LV.cellml) is merged with the model of the ascending aorta (ascending\_aorta\_C0.cellml). Time ( $t$ ) and the amount of the flow ( $v_{LV}$ ) in the LV.cellml module are mapped to the time ( $t$ ) and the source of flow ( $Sf_{in}$ ) variables in the ascending\_aorta\_C0.cellml module. The grey lines show the internal dependencies between the variables in each module and the orange and blue lines show the links between the modules.

We started the model composition by creating the input to the system, which was 244  
generating the output flow of the heart left ventricle. The flow wave was obtained from 245  
digitising the analogous signal in the whole heart model, previously created in the 246  
ADAN closed-loop system [25]. The fitting task was performed in MATLAB, using a 247  
two-term Gaussian function as in Eq (8) with the settings shown in S1 Table. 248

$$f(x) = \sum_{i=1}^2 a_i e^{-\left(\frac{x-b_i}{c_i}\right)^2} \quad (8)$$

The digitised flow was imposed to both the newly merged model and the manually composed (ADAN open-loop) model in CellML for 10 seconds (S2 Fig).

To compare the simulation results between the two approaches, normalised root mean square error (NRMSE) was also computed for each set of results as in Eq (9), where  $\hat{y}_i$  corresponds to the simulation points of our composed model using SemGen, and  $y_i$  corresponds to the original ADAN open-loop simulation points. The normalisation was done relative to the difference of maximum and minimum data of the reference model (ADAN open-loop) in each simulation.

$$NRMSE = \frac{\sqrt{\sum_{i=1}^n \frac{(\hat{y}_i - y_i)^2}{n}}}{y_{max} - y_{min}} \quad (9)$$

## Results

We applied our hierarchical semantic model composition method to the bond graph ADAN model downloaded from the *Cardiovascular Circulation Workspace* on PMR (Physiome Model Repository). Thereafter, modules were extracted and modified to create templates (as described in Template modules section). Creating all the vessel segments from these templates, the modules were annotated and coupled using SemGen. The output model was then imported to OpenCOR (an environment to simulate CellML models: [www.opencor.ws](http://www.opencor.ws)). The final composed model is available at <https://github.com/NilooFar-Sh/ADAN-86-Bond-Graph-Model-Composition>.

The aim of our approach is to show that the ADAN model equations can be generated using automated semantic composition. Here, we compare the simulation results of our approach with the existing ADAN open-loop model. After reaching steady-state, blood flow and pressure were plotted from  $t = 9$  s to  $t = 10$  s. The results from the two models are compared in Fig 11 and Fig 12. The plots show an almost exact match between the results of the two modelling approaches, indicating that the semantically composed model closely approximates the ADAN model. The minor differences that arise are due to the limbs' symmetrical nature, whereas the original ADAN model used separate parameters for the left and right limbs.

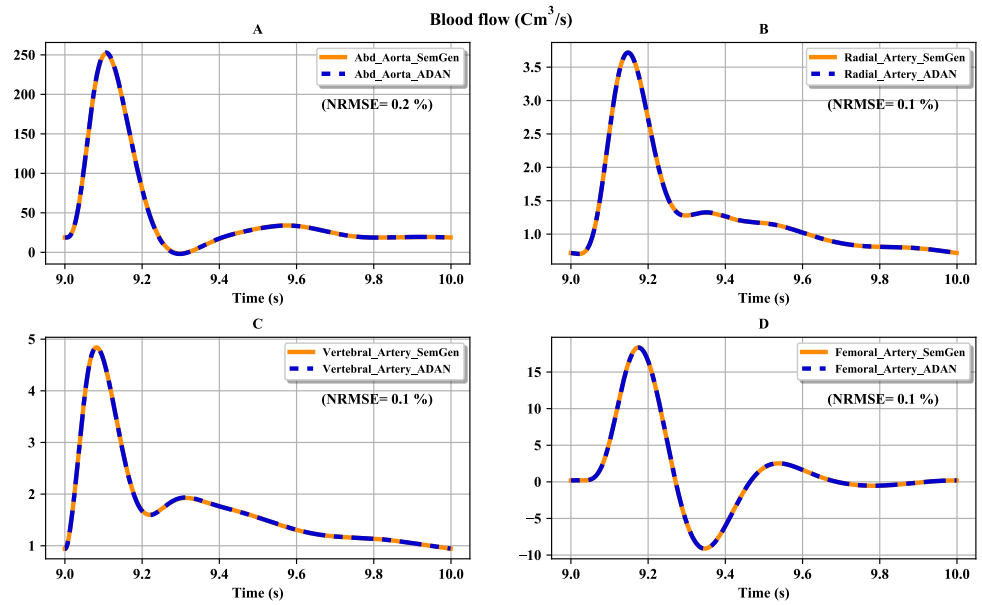


**Fig 11. Comparison between the flows obtained from the ADAN open-loop model and our version of the model.** (A) Flow in the abdominal aorta; (B) flow in the radial artery; (C) flow in the vertebral artery; (D) flow in the femoral artery. The normalised root mean square errors (NRMSE) are represented as percentages.

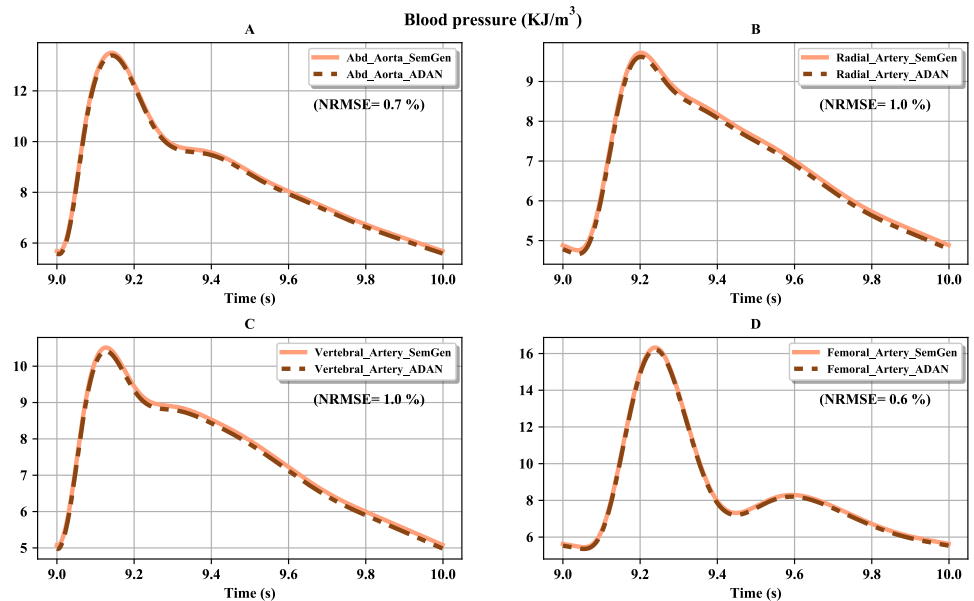


**Fig 12. Comparison between the pressures obtained from the ADAN open-loop model and our version of the model.** (A) Pressure in the abdominal aorta; (B) pressure in the radial artery; (C) pressure in the vertebral artery; (D) pressure in the femoral artery. The normalised root mean square errors (NRMSE) are represented as percentages.

## Discussion

In this paper, we introduced a general method for assembling models from templated modules, demonstrated with the ADAN open-loop arterial model. This was done by encoding bond graph sub-models in CellML and using the annotation-based merging tool of SemGen to construct the system model using semantic annotations. Having the sub-models represented as bond graphs has allowed us to systematically compose a model from a large number of modules. Furthermore, enriching the modules with biological semantics assists us in coupling them. In the case where the system has similar sections consisting of several modules (here we have symmetric limbs in the ADAN open-loop model), a hierarchical approach to model composition can be utilised. Once a section is composed, other similar sections can be created by generating copies of that section.

Simulation results were compared to the ADAN open-loop model. The slight differences in the flow and pressure of the vessels in the two models originate from the fact that unlike the original ADAN model, similar limbs were considered identical. Supposing that similar limbs are identical and exactly have the same vessel segments and parameter values, the modules for one limb were merged, and this integrated model was copied and used for the other limb as well (both for arms and legs). This significantly accelerated the process of merging models at the expense of minor differences in simulation results. Even if this simplification is not made and each limb segments are coupled individually, still the model composition procedure remains fast and more reliable than editing the CellML code directly in complex biological systems.

Currently, SemGen does not allow importing other CellML models to the main model; for example, in [25], the list of required units (*Units.cellml* module) was imported to the *main.cellml* model. Thus, in our recreated model, all the required units were defined in the same file in which each module was defined. We expect this file importing feature will be added to SemGen in the near future. Although the current composition method is more convenient and faster compared to time-consuming and error-prone manual merging, it does require adding extra variables to the modules and managing the mappings between the biological annotations in SemGen. According to the long-term goals presented for SemGen, the capability of equation modification in

the case of merging two models will be added [41]. This will enable the reuse of the existing modules without needing to add such extra variables.

This approach can also be utilised in other domains of application, for example cellular biochemistry, where different modules of biochemical reactions couple together and represent a biological pathway or network. Bearing in mind that one biochemical species can be both produced in one reaction and consumed by another reaction, the rate of molar change for each species would be the summation of multiple reaction rates. By adding and annotating auxiliary variables to the constitutive equations in each module, a number of ports for model composition will be available. The idea of manual ‘white box’ composition of bond graph models of biochemical systems has previously been explored by Gawthrop [20] where a modular bond graph model of mitochondrial electron transport chain was developed. Gawthrop et al. [50] have also described a reusable and modular model of glycogenolysis in skeletal muscle. Our work expands on these approaches through the addition of the biological semantics, which enables the automation of model composition.

## Conclusion

We have utilised the the SemGen annotator and merger tools to create a composed model of artery segments based on the ADAN open-loop model. Describing the vessel segments in terms of bond graphs helped us avoid post-merging adjustments in the model equations (as is almost always necessary in dealing with conventional computational models). The bond graph framework facilitates the procedure of extending biological and physiological models with minimal error and effort. Also, using the SemGen merger tool for coupling the modules allowed us to skip the manual code-wise mappings between the modules in CellML. We anticipate that our approach will enable future work on constructing multiscale models of organs that bridge biochemical processes at the cellular level to tissue-level processes such as circulation.

## Acknowledgments

332

NS would like to thank Maxwell Neal, Keri Moyle, and Anand Rampadarath for their helpful comments and suggestions.

333

334

All the authors have revised and provided the final approval of the submitted manuscript.

335

336

## References

1. ReKate HL, Brodkey JA, Chizeck HJ, et al. Ventricular volume regulation: A mathematical model and computer simulation. *Pediatr Neurosci*. 1988; 14(2): 77–84. doi: 10.1159/000120367.
2. Voronova V, Sokolov V, Al-Khaifi A, et al. A physiology-based model of Bile acid distribution and metabolism Under healthy and pathologic conditions in human beings. *Cell Mol Gastroenterol Hepatol*. 2020; 10(1): 149–170. doi: 10.1016/j.jcmgh.2020.02.005.
3. Neal ML, Cooling MT, Smith LP, et al. A Reappraisal of how to build modular, reusable models of biological systems. *PLoS Comput Biol*. 2014 Oct; 10(10): e1003849.
4. Gawthrop PJ, Cudmore P, Crampin EJ. Physically-plausible modelling of biomolecular systems: A simplified, energy-based model of the mitochondrial electron transport chain *J. Theor. Biol*. 2020 May; 493: 110223-. doi: 10.1016/j.jtbi.2020.110223.
5. Cooling MT, Hunter P, Crampin EJ. Modelling biological modularity with CellML. *IET Syst Biol*. 2008 Mar; 2(2): 73–9. doi: 10.1049/iet-syb:20070020.
6. Cobos Méndez R, de Oliveira Filho J, Dresscher D, et al. A bond-graph metamodel: physics-based interconnection of software components. In: Arbab F, Jongmans SS, editors. *Formal Aspects of Component Software*. Lecture Notes in Computer Science, vol 12018. Springer, Cham. 2020. pp 87–105. doi: 10.1007/978-3-030-40914-2\_5.

7. Choi YD, Goodall JL, Sadler JM, et al. Toward Open and Reproducible Environmental Modeling by Integrating Online Data Repositories, Computational Environments, and Model Application Programming Interfaces. *Environ Model Softw*. 2020 Oct. doi: 10.1016/j.envsoft.2020.104888.
8. Hurley DG, Budden DM, Crampin EJ. Virtual reference environments: a simple way to make research reproducible. *Briefings in Bioinformatics* 2015, 16 (5) 901–903.
9. Kohl P, Crampin EJ, Quinn TA, et al. Systems biology: An approach. *Clin Pharmacol Ther*. 2010 Jul; 88(1):25–33.
10. Schölzel C, Blesius V, Ernst G, et al. The impact of mathematical modeling languages on model quality in systems biology: A software engineering perspective. *bioRxiv*. 2020 Jul; doi: 10.1101/2019.12.16.875260.
11. Fischer HP. Mathematical modeling of complex biological systems: From parts lists to understanding systems behavior. *Alcohol Res Health*. 2008; 31(1):49–59. PMID: 23584751; PMCID: PMC3860444.
12. Birtwistle MR, Mager DE, Gallo JM. Mechanistic vs. empirical network models of drug action. *CPT Pharmacometrics Syst Pharmacol*. 2013 Sep; 2(9): e72.
13. Crampin EJ, Smith NP, Hunter PJ. Multi-scale modelling and the IUPS Physiome project. *J Mol Histol*. 2004 Sep; 35(7):707–714. doi: 10.1007/s10735-004-2676-6.
14. Hunter P. The virtual physiological human: The Physiome project aims to develop reproducible, multiscale models for clinical practice. *IEEE Pulse*. 2016 July-Aug; 7(4): 36–42. doi: 10.1109/MPUL.2016.2563841.
15. Zhang H. A knowledge enriched computational model to support lifecycle activities of computational models in smart manufacturing. PhD Thesis, Syracuse University, College of Engineering & Computer Science. 2018. Available from: <https://surface.syr.edu/etd/947>.

16. Cooling MT, Crampin EJ, Hunter PJ. Physiome mark-up languages for systems biology: model modularization and re-use. *Systems Biomedicine*. 2010. p. 315-328. doi: 10.1016/B978-0-12-372550-9.00013-4.
17. Hunter PJ, Crampin EJ, Nielsen P MF. Bioinformatics, multiscale modelling and the IUPS Physiome project. *Brief Bioinform*. 2008 May; 9(4):333–343. doi: 10.1017/S0033583506004227.
18. Rudy Y, Silva JR. Computational biology in the study of cardiac ion channels and cell electrophysiology. *Q Rev Biophys*. 2006 Feb; 39(1):57–116.
19. Pan M. A bond graph approach to integrative biophysical modelling. PhD Thesis, The University of Melbourne, Melbourne School of Engineering, Department of Biomedical Engineering. 2019. Available from: <https://minerva-access.unimelb.edu.au/handle/11343/230908>.
20. Gawthrop PJ. Bond graph modeling of chemiosmotic biomolecular energy transduction. *IEEE Trans Nanobioscience*. 2017 Apr; 16(3): 177–188. doi: 10.1109/TNB.2017.2674683.
21. de Bono B, Safaei S, Grenon P, et al. Meeting the multiscale challenge: representing physiology processes over ApiNATOMY circuits using bond graphs. *Interface Focus*. 2017 Dec. 8(1): 20170026. doi: 10.1098/rsfs.2017.0026.
22. Gawthrop PJ, Crampin EJ. Energy-based analysis of biochemical cycles using bond graphs. *Proc R Soc A*. 2014 Nov; 470: 20140459. doi: 10.1098/rspa.2014.0459.
23. Pan M, Gawthrop PJ, Tran K, et al. A thermodynamic framework for modelling membrane transporters. *J Theor Biol*. 2019 Nov; 481: 10–23. doi: 10.1016/j.jtbi.2018.09.034.
24. Paynter HM. Analysis and design of engineering systems. MIT Press. 1961.
25. Safaei S, Blanco PJ, Müller LO, et al. Bond graph model of cerebral circulation: Toward clinically feasible systemic blood flow simulations. *Front Physiol*. 2018 Mar; 9:148. doi: 10.3389/fphys.2018.00148.



26. Oster G, Perelson A, Katchalsky A. Network thermodynamics. *Nature*. 1971 Dec; 234: 393–399. doi: 10.1038/234393a0.
27. Neal ML, König M, Nickerson D, et al. Harmonizing semantic annotations for computational models in biology. *Brief Bioinform*. 2019 Mar; 20(2): 540–550. doi: 10.1093/bib/bby087.
28. Fontaine G, Hammami O. Automatic model search for system model composition. 2018 IEEE International Systems Engineering Symposium (ISSE). 2018 Nov; doi: 10.1109/SysEng.2018.8544449.
29. Haav HM, Ojamaa A. Semi-automated integration of domain ontologies to DSL meta-models. *Int J Intell Inf Database Syst*. 2017 Jan; 10(1/2): 94–116. doi: 10.1504/IJIIDS.2017.086198.
30. Matos E, Campos F, Braga R, et al. CelOWS: An ontology based framework for the provision of semantic web services related to biological models. *J Biomed Inform*. 2010 Feb; 43(1): 125–136. doi: 10.1016/j.jbi.2009.08.008.
31. Pan M, Gawthrop PJ, Tran K, et al. Bond graph modelling of the cardiac action potential: implications for drift and non-unique steady states. *Proc R Soc A*. 2018 Jun; 474(2214): 20180106. doi: 10.1098/rspa.2018.0106.
32. Sarwar DM, Kalbasi R, Gennari JH, et al. Model annotation and discovery with the Physiome Model Repository. *BMC Bioinformatics*. 2019 Sept; 20: 457. doi: 10.1186/s12859-019-2987-y.
33. Cuellar AA, Lloyd CM, Nielsen PF, et al. An overview of CellML 1.1, a biological model description language. *Simulation*. 2003 Dec; 79(12): 740–747.
34. Hucka M, Finney A, Sauro HM, et al. The systems biology markup language (SBML): a medium for representation and exchange of biochemical network models. *Bioinformatics*. 2003 Mar; 19(4): 524–531.
35. Neal ML, Carlson BE, Thompson CT, et al. Semantics-based composition of integrated cardiomyocyte models motivated by real-world use cases. *PLoS ONE*. 2015 Dec; 10(12): e0145621. doi: 10.1371/journal.pone.0145621.

36. Butterworth E, Jardine BE, Raymond GM, et al. JSim an open-source modelling system for data analysis. *F1000research*. 2013 Dec; 2:288. doi: 10.12688/f1000research.2-288.v1.
37. Neal ML, Thompson CT, Karam GK, et al. SemGen: a tool for semantics-based annotation and composition of biosimulation models *Bioinformatics*. 2019 May; 35(9):1600–1602. doi: 10.1093/bioinformatics/bty829.
38. Safaei S, Bradley CP, Suresh V, et al. Roadmap for cardiovascular circulation model. *J Physiol*. 2016 Aug;594(23):6909–6928.
39. Watanabe SM, Blanco PJ, Feijóo RA. Mathematical model of blood flow in an anatomically detailed arterial network of the arm. *ESAIM: M2AN*. 2013 Jun; 47(4): 961–985. doi: 10.1051/m2an/2012053.
40. Beard DA, Neal ML, Tabesh-Saleki N, et al. Multiscale modelling and data integration in the Virtual Physiological Rat project *Ann Biomed Eng*. 2012 Nov; 40(11): 2365–2378.
41. Neal ML. Long term SemGen goals. 2019 May 19. In: GitHub [Internet]. Available from: <https://github.com/SemBioProcess/SemGen/wiki/Long-term-SemGen-goals>
42. Gennari JH, Neal ML, Galdzicki M, et al. Multiple ontologies in action: Composite annotations for biosimulation models. *J Biomed Inform*. 2011 Feb; 44(1):146–154.
43. Shi Y, Korakianitis T. Impeller-pump model derived from conservation laws applied to the simulation of the cardiovascular system coupled to heart-assist pumps. *Comput Biol Med*. 2018 Feb; 93:127–138. doi: 10.1016/j.compbimed.2017.12.012.
44. Gawthrop PJ, Crampin EJ. Modular bond-graph modelling and analysis of biomolecular systems *IET Syst Biol*. 2016 Jun; 10(5):187–201.
45. Díaz-Zuccarini V, Pichardo-Almarza C. On the formalization of multi-scale and multi-science processes for integrative biology *Interface Focus*. 2011 Jun;1(3):426–37. doi: 10.1098/rsfs.2010.0038.

46. Smith LSPS. Bond graph modelling of physical systems PhD Thesis, The Faculty of Engineering of Glasgow University. 1993. Available from: <http://theses.gla.ac.uk/74811/1/11007730.pdf>
47. Gawthrop PJ, Smith LPS. Metamodelling: Bond graph and dynamic systems 1st ed. Prentice Hall International (UK) Limited; 1996.
48. Podesser BK, Neumann F, Neumann M, et al. Outer radius-wall thickness ratio, a postmortem quantitative histology in human coronary arteries. *Acta Anat.* 1998 July; 163(2): 63–8. doi: 10.1159/000046485.
49. Xiaomei G, Xiao L, Huimin R, et al. Estrogen modulates the mechanical homeostasis of mouse arterial vessels through nitric oxide. *Am J Physiol Heart Circ Physiol.* 2006 May; 290(5): H1788–97. doi: 10.1152/ajpheart.01070.2005.
50. Gawthrop PJ, Cursons J, Crampin EJ. Hierarchical bond graph modelling of biochemical networks. *Proc. R. Soc. A.* 2015 Dec; 471: 20150642. doi: 10.1098/rspa.2015.0642.

## Supporting information

**S1 Table. MATLAB fitting tool settings and estimated parameters in digitising the cardiac output flow.** The fitting options which are not mentioned in the table are remained untouched as their default values in the MATLAB fitting tool.

**S2 Fig. The digitised cardiac output flow.** The yellow line and dashed red line show the same imposed flow in the SemGen merged model and the ADAN open-loop model.